ACS OMEGA

Open Access

http://pubs.acs.org/journal/acsodf

Article

Construction of an Interfacial Layer of Aramid Fibers Grafted with Glycidyl POSS Assisted by Heat Treatment and Evaluation of Interfacial Adhesion Properties with Epoxy Resin

Yang Li, Caiwen Shi, Xiaoli Pan, Ziyi Wang, and Le Yang*

Cite This: *ACS Omega* 2024, 9, 24489−24499

Read Online

ACCESS | Metrics & More | Article Recommendations

ABSTRACT: The surface of para-aramid fibers (AFs) was modified via air-assisted heat pretreatment and solution impregnation by varying the glycidyl polyhedral oligomeric silsesquioxane (POSS) content. Fourier transform infrared spectroscopy and X-ray photoelectron spectroscopy showed an ester group, confirming the graft reaction between glycidyl POSS and oxidized AFs. The mechanical properties of AFs could be altered by varying the glycidyl POSS content. The modified AFs exhibited an optimal tensile strength after embedding 5 wt % glycidyl POSS on the fiber surface. The thermal stability of the modified fibers decreased; however, no obvious changes in crystallinity were observed by varying the glycidyl POSS content. Moreover, the tensile strength of monofilament increased from 23.8 to 25.8 cN·dtex^{-1}, the thickness of the grafted layer on the fiber surface was above 30−40 nm after the graft modification with 5 wt % glycidyl POSS, and the interfacial shear strength (IFSS) increased by 62.55% to 26.22 MPa. Thus, the modified glycidyl AFs can be used for the reinforcement of composite materials.

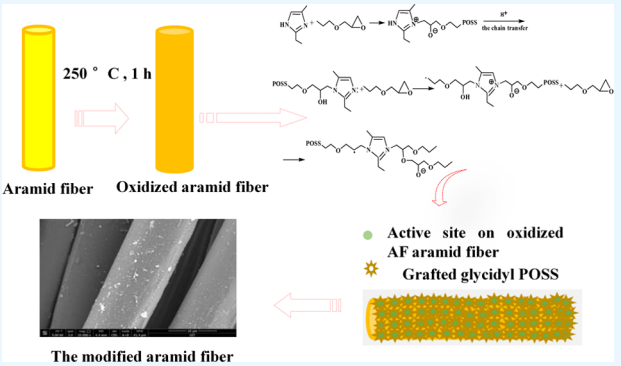

1. INTRODUCTION

Para-aramid fibers (AFs) exhibit high performance and excellent properties such as high modulus, low specific density, electrical conductivity, and high tensile strength.[1] AF-reinforced resin composites are widely used in many applications in many spheres, such as aerospace components, auto parts, sports products, and pressure vessels, owing to the superior strength of AFs and matrix resin.[2,3] However, AFs have poor interfacial adhesion and compatibility with the resin matrix owing to their smooth and chemically inert surface.[4,5] To improve the surface chemical activity of AFs and their interfacial adhesion with matrix materials, various surface modification techniques have been used, including chemical grafting,[6−8] chemical etching,[9] high-energy irradiation,[10,11] and physical coating.[12,13] However, these conventional treatment methods deteriorated the fiber strength.[14] Moreover, due to their excessive chemical stability, the AFs showed high inertness to chemical grafting and physical coating.[15,16]

Nanoscale modifying agents that can impact the desirable structural and functional properties of AFs are widely studied owing to their high dispersibility and functional group activity.[17] Glycidyl polyhedral oligomeric silsesquioxanes (POSSs) have a unique cage-like molecular structure with an internal inorganic silicon−oxygen framework surrounded by organic substituents that endow them with high polarity and compatibility. The introduction of glycidyl POSS nanoparticles in AFs can improve their mechanical properties and compatibility.[18,19] However, the formation of an aggregated structure and a grafted layer on the AF surface after modification has not yet been investigated. Moreover, grafting glycidyl POSSs onto AFs is challenging because of the absence of reactive sites on the fiber surface.

Glycidyl POSSs can adhere to the AF surface via a physical adhesion process; however, the process is time-consuming, and glycidyl POSS oligomers tend to form aggregates via noncovalent interactions, resulting in a loose and heterogeneous coating that considerably weakens the adhesion strength in composite materials.[20] Plasma oxidation is an effective strategy for enhancing the surface polarity of AFs without affecting their surface properties.[21] Plasma oxidation promotes adhesion by increasing the surface polarity after the introduction of functional groups such as COOH, Ph−OH, and CO, particularly for AFs[21] and carbon fibers.[22,23] Air thermal oxidation is also used for surface modification, which catalyzes the oxidation of AFs to improve their surface

Received: January 11, 2024
Revised: May 17, 2024
Accepted: May 23, 2024
Published: May 29, 2024

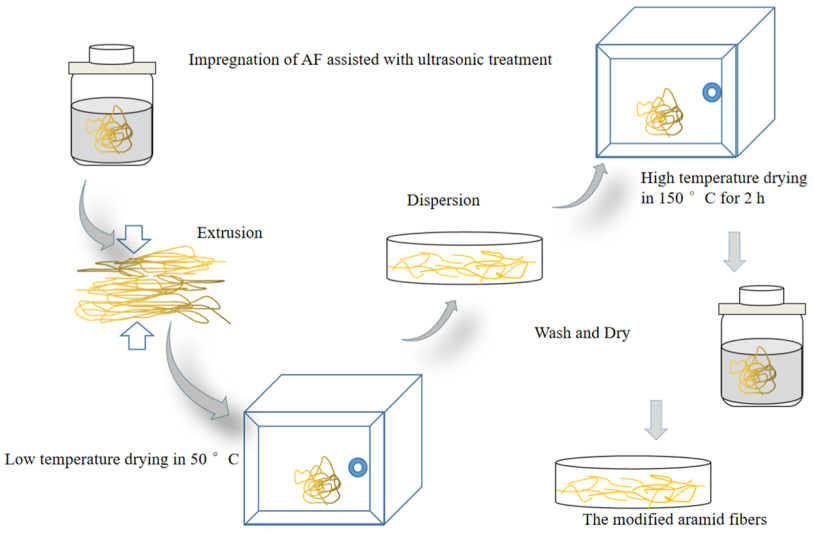

Figure 1. Schematic of glycidyl POSS grafting modification.

polarity.[12,24] The surface hydrogen bonds of AFs can be reconstructed and partially oxidized via heat treatment.[25] Our previous research confirmed that the molecular chain on the AF surface was oxidized, and part of C−H was oxidized into polar groups such as −OH and −COOH during heat treatment.[26] The increase in the number of polar groups creates favorable conditions for chemical graft modification and coating of polyamide acid (PAA). On the basis of our previous research, a novel and effective approach to graft glycidyl POSSs onto AFs using a high-heat treatment process was proposed herein. In order to make a systematic comparison with the previous research, two comparisons, protofilament fiber and heat-treated fiber, named AF0 and AFt, respectively, were introduced for comparison in this study. The surface morphology, aggregation structure, and thermal performance of modified AFs and the interfacial properties of the epoxy/AF composites were systematically investigated.

2. METHODS

2.1. Materials. Glycidyl POSS (EP0409, Hybrid Plastics), epoxy resin (EP, E-44, ShangHai Resin Factory Co., Ltd.), 2-ethyl-4-methylimidazole (2E4MZ, Shikoku Chemical Industry Co., Ltd.), AFs (AF-1000, 1500D; South, Alkex Company, Korea), and acetone (AR, Chongqing Chuan Dong Chemical Co., Ltd.) were used as raw materials.

2.2. Preparation of Modified AFs. *2.2.1. Pretreatment of AFs.* Before modification, AFs were first cleaned with acetone for 20 min to remove the sizing agent on the fiber surface and then dried at 80 °C for 2 h. AFs were pretreated via thermal oxidation treatment as follows: A certain amount of AFs was placed in an air-drying oven. The oven was rapidly heated to 250 °C and treated under a constant temperature for 1 h. After reaching the set time, the fibers were removed and sealed for use. The pretreated fibers were labeled AFt.

2.2.2. Preparation of POSS-Modified AF Samples. The schematic diagram of the glycidyl POSS grafting modification process is shown in Figure 1. Glycidyl POSS mixed with 4% 2E4MZ (as an accelerant) was diluted with acetone to a specific concentration (1, 3, 5, 7, and 9%), placed in a beaker with oxidized AFs for 10 min (100 mL of glycidyl POSS solution, 0.5 g AF), and removed. The excess solvent was removed from the surface via extrusion, and heat treatment was performed in an oven at 150 °C for 2 h. During the heat treatment, the AF bundles were turned over and dispersed to prevent formation of fiber bundles. After surface modification, the samples were taken out, washed with acetone to remove the unreacted glycidyl POSS on the AF surface, and dried (Table 1). The reaction mechanism of AF grafting modification with glycidyl POSS is presented in Figure 2.

Table 1. Sample Numbers and Treatment Process

sample numbers	treatment process
AF0	untreated
AFt	oxidized aramid fiber (heat treatment at 250 °C for 1 h)
AFt-1	oxidized aramid fiber (AFt) was soaked in a 1% glycidyl POSS solution at 25 °C for 10 min and then dried at 150 °C for 2 h
AFt-3	oxidized aramid fiber (AFt) was soaked in a 3% glycidyl POSS solution at 25 °C for 10 min and then dried at 150 °C for 2 h
AFt-5	oxidized aramid fiber (AFt) was soaked in a 5% glycidyl POSS solution at 25 °C for 10 min and then dried at 150 °C for 2 h
AFt-7	oxidized aramid fiber (AFt) was soaked in a 7% glycidyl POSS solution at 25 °C for 10 min and then dried at 150 °C for 2 h
AFt-9	oxidized aramid fiber (AFt) was soaked in a 9% glycidyl POSS solution at 25 °C for 10 min and then dried at 150 °C for 2 h

2.3. Surface Chemical Composition Analysis. The surface chemical composition of modified AFs was analyzed by X-ray photoelectron spectroscopy (XPS) measurement on a Thermo Kα+ system (Thermo Fisher Scientific) equipped with an Mg Ka X-ray source and a pass energy of 1486.6 eV. X-ray diffraction (XRD) analyses were performed using a diffractometer with the type X Pert PRO (Panalytical, the Netherlands). Test conditions were set as follows: Cu−Ka radiation, a tube voltage of 40 kV, and a tube current of 40 mA. The scan range was 10−40°, with a scan rate of 2°/min. The microstructure of the samples was studied by using field emission scanning electron microscopy (Sirion 200, FEI). The surface topography of modified AFs was observed via atomic force microscopy (AFM) on a dimension icon atomic force microscope (Bruker, Germany). Tapping mode was used, and each AFM image was analyzed for their average surface roughness (R_a) and root-mean-square roughness (R_q) in a 3 × 3 μm^2 area. Tapping mode was used, and each AFM image was analyzed in terms of surface average roughness (R_a) and root-

https://doi.org/10.1021/acsomega.4c00260
ACS Omega 2024, 9, 24489−24499

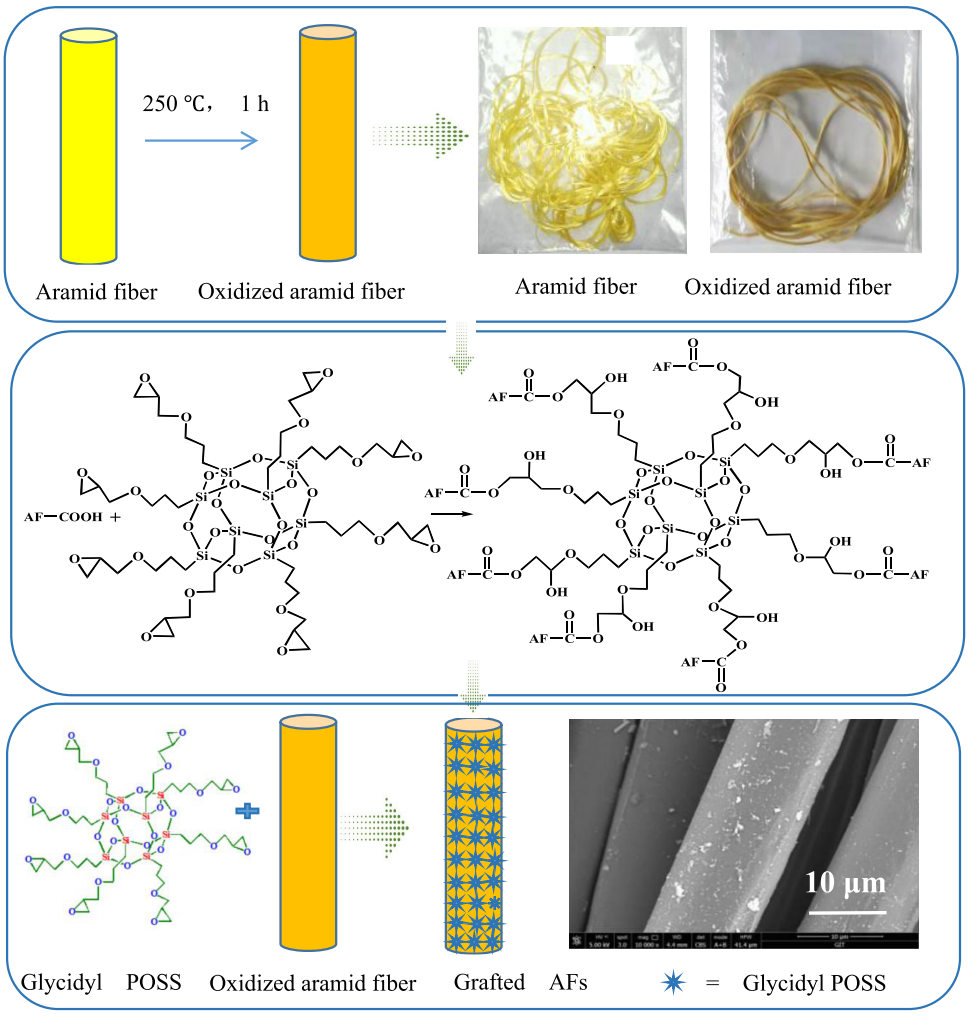

Figure 2. Reaction mechanism of AF grafting modification with glycidyl POSS.

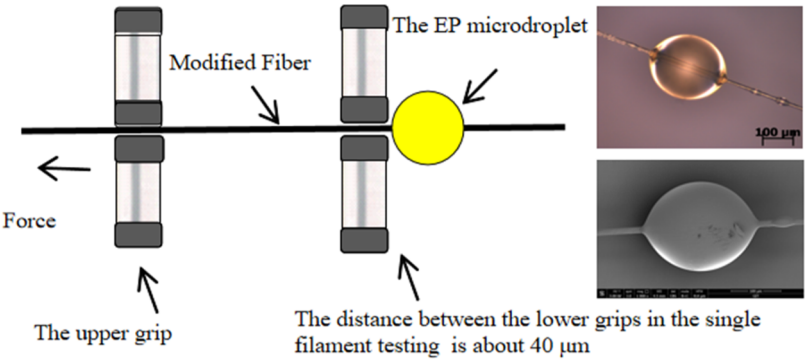

Figure 3. Schematic of the AF/EP droplet test.

mean-square roughness (R_q) of 3 × 3 μm^2 area. R_a is the arithmetic average of the absolute value of the height deviation in the region of 3 × 3 μm^2, and R_q is the root-mean-square value of the deviation of the contour from the mean line in this region. R_a and R_q values are calculated by the test software.

2.4. Grafting Interface Layer Characterization. The EP curing system contained EP E-44 and 4 wt % 2E4MZ as the curing agent. A single modified AF was placed in the EP matrix and soaked completely, followed by heat treatment in a vacuum oven for 1 h at 150 °C for curing. Before the test, the pattern was sliced at room temperature with a Leica UC7 slicing instrument, Leica UC7. The slice was 70−90 nm thick, and the slicing speed was 1.8 mm/s. Then, the samples were scanned using a transmission electron microscope (Jeol-1230, Japan).

2.5. Fiber Tensile Test. To investigate the effect of heat treatment on the tensile properties of AFs, the tensile strengths of AFs before and after modification were tested on an ASTM-D3379 single filament testing device (Shanghai New Fiber Instrument Co., Ltd., XQ-1, China). The modified fibers were conditioned for at least 24 h at 20 °C and a relative humidity of 65% prior to tensile testing. Due to a large standard

https://doi.org/10.1021/acsomega.4c00260
ACS Omega 2024, 9, 24489−24499

deviation in the tensile characteristics, at least 50 fibers were tested for each set of samples.

2.6. Adhesion Measurement. The single fiber pull-out test was used to characterize the interfacial properties of AF/epoxy (AF/EP) composites on the single filament testing device XQ-1 (Shanghai New Fiber Instrument Co., Ltd., China). Figure 3 schematizes the AF/EP droplet test. The specimens were prepared as follows. A drop of EP was added to the AF surface using a needle. Then, the AF/EP microdroplet samples were moved into an oven for heat treatment. After the specimens were placed in the oven, the bottom fixture was adjusted for the AF to adhere to the EP microdroplets at the bottom. The upper clamping device clamped the fiber, and a steady displacement was applied to remove the single fiber from the droplets at a displacement rate of 10 mm/min. The diameter (D) and embedding length (L) of the fibers were measured using the inverted metallographic microscope (Axio Observer Z1m, Zeiss, Germany). The test was conducted at room temperature, and the maximum load was measured. For each group, 50 samples were tested and averaged. Assuming the IFSS was approximately constant along the entire interface, the average IFSS was calculated using eq 1

$$\Gamma = \frac{Fd}{\pi DL} \tag{1}$$

where Γ is the average IFSS, F_d is the maximum load of interfacial failure, D is the fiber diameter, and L is the embedded length.

3. RESULTS AND DISCUSSION

3.1. FTIR Analysis. The graft reaction during surface modification was verified via Fourier-transform infrared (FTIR) characterization (Figure 4). As we previously reported, the FTIR spectrum of the control specimen (AF0) shows characteristic peaks of AFs at 3296 cm^{-1} corresponding to the hydrogen bond association state of −NH, 1647 cm^{-1} corresponding to the stretching vibration of −C═O for the amide I band, 1539 cm^{-1} corresponding to the curved vibration of −N−H, and 1307 cm^{-1} corresponding to the bending vibration of −N−H.[26] However, the characteristic peaks of the C−H bond at 2920 and 2850 cm^{-1} disappear, indicating the decomposition of the graft layer on AFt. Meanwhile, new characteristic bands appear at 1260, 1610, and 1726 cm^{-1}, which confirmed the oxidation of benzene rings on the surface molecular chain during heat treatment.[12,27] The peaks at 2920 and 2850 cm^{-1} reappeared after the graft reaction of glycidyl POSS, corresponding to the $-CH_2-$ structure of the glycidyl POSS molecular chain, indicating the occurrence of the graft reaction.[17,25,26]

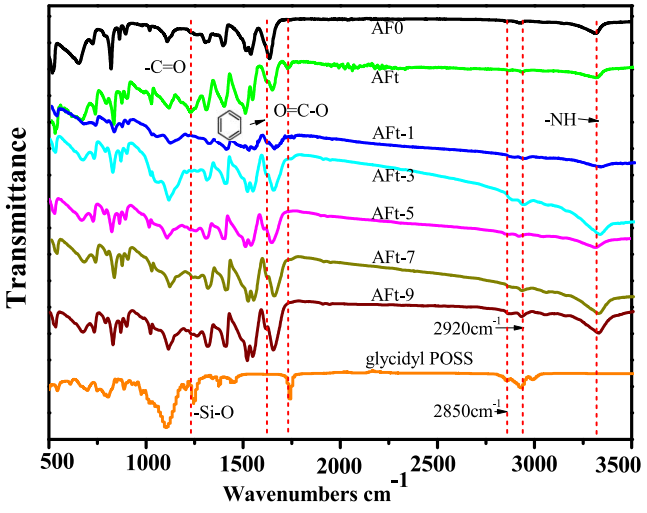

Figure 4. FTIR spectra of AFs modified with glycidyl POSS (AF0 and AFt have been reprinted from refs 26,27., Pages No Copyright (2024) with permission from Elsevier).

3.2. XPS Analysis. XPS is used to analyze the changes in the surface chemical composition, including elements and functional groups, induced by surface modification. The wide scan and C 1s core-level XPS spectra of AFs before and after modification are shown in Figure 5, and the XPS results of the surface elemental composition of modified AFs with varying glycidyl POSS contents are shown in Tables 2 and 3. Due to the presence of a sizing agent, the control sample (AF0) surface contained 77.16, 12.12, and 10.72% of C, O, and N, respectively; the content of O was slightly higher than that of N (Table 1).[12,20] As reported in our previous analysis, the O element concentration increased from 12.12 to 15.68% for AFt after the oxidation in heat treatment.[26] With the grafting of glycidyl POSS, the O concentration increased to 15.98% for AFt-5, indicating glycidyl POSS grafting on the fiber surface. With the dosages increasing, the O and N concentrations increased and decreased, respectively. After modification, the O concentrations were 15.02, 15.98, and 15.64% for AFt-3, AFt-5, and AFt-7, respectively, indicating more and more glycidyl POSS grafting or coating on the modified fibers.[13,26,27]

The XPS deconvolution analysis of C 1s peaks was performed to examine the changes in the functional side group. The shapes of C 1s peaks of all of the modified fibers were different from those of the control fiber (AF0). The C 1s spectrum of AF0 showed four peaks at binding energies of ∼284.5, 285.3, 286.3, and 288 eV assigned to C−C, C═C, C−N, and C═O, respectively.[12,13,24] After oxidation treatment (Figure 5b), the C 1s peak was fitted to an obvious peak at ∼289 eV, indicating the generation of −COOH on the fiber surface. In contrast to AFt, the curved-fitted peak of −COO− (289 eV) for the modified fibers, derived from the reaction of the epoxy terminal group of glycidyl POSS with −OH or −COOH produced during heat treatment, became increasingly obvious (Figure 5c−e). The −COO− concentration steadily increased, indicating that large amounts of glycidyl POSS were grafted on the modified fiber surface.[21,26,27] When the AF surface was modified with 5% glycidyl POSS (Figure 5d), the −COO− concentration increased to a maximum value of 2.41%. Surface modification by glycidyl POSS assisted with oxidation pretreatment depended on the free radical concentration.[28] The number of polar groups produced during oxidation pretreatment on the surface of the fiber is limited. After modification with 7% glycidyl POSS, the −COO− content was 1.93%, lower than that of AFt-5.

3.3. Surface Aggregated Structure Analysis. Figure 6 presents the XRD pattern of aramid fiber grafted with different dosages of glycidyl POSS. AFs are highly aligned crystalline materials with 2θ = 20.06, 28.2, and 21.37° corresponding to (110), (200), and (004) planes, respectively.[26,31] As shown in Figure 6, there is no obvious diffraction peak in each sample, but the diffraction angle and the relative area of the two main diffraction peaks have obvious changes. The XRD patterns for each sample were determined using the curve fitting and

https://doi.org/10.1021/acsomega.4c00260
ACS Omega 2024, 9, 24489−24499

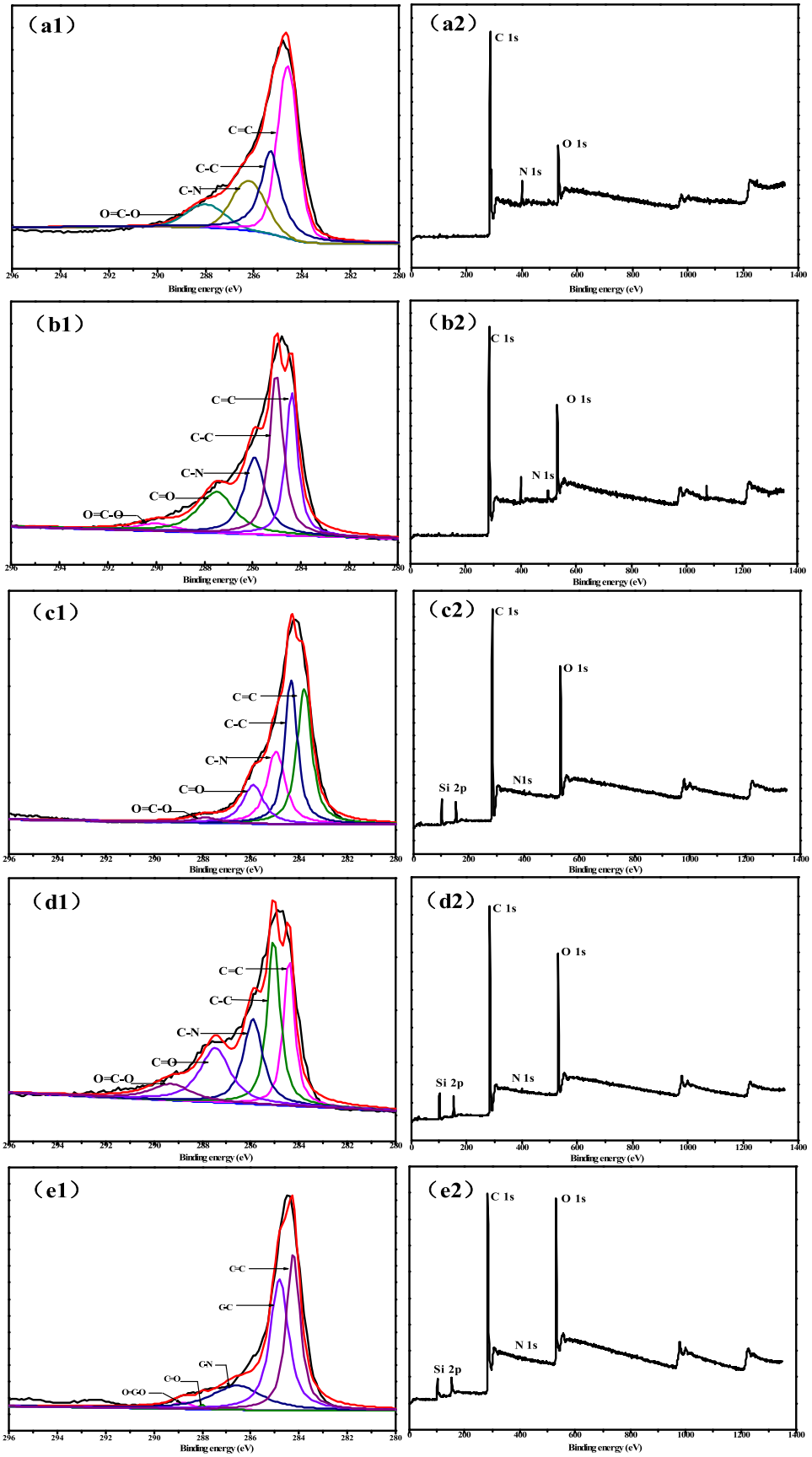

Figure 5. XPS spectra of modified AFs (AF0 and AFt have been reprinted from refs 26,27., Pages No Copyright (2024) with permission from Elsevier). a1, a2—AF0; b1, b2—AFt; c1, c2—AFt-3; d1, d2—AFt-5; e1, e2—AFt-7.

https://doi.org/10.1021/acsomega.4c00260
ACS Omega 2024, 9, 24489−24499

Table 2. Relative Chemical Compositions and Atomic Ratios Determined by XPS before and after Modifying (AF0 and AFt have been Reprinted from Refs 26,27., Pages No Copyright (2024) with Permission from Elsevier

	chemical composition (%)				atomic ratio	
sample	C	O	N	Si	C/N	O/N
AF0	77.16	12.12	10.72	0	6.36	1.13
AFt	73.89	15.68	10.43	0	7.08	1.50
AFt-3	73.02	15.02	9.14	2.82	7.98	1.64
AFt-5	72.49	15.98	6.28	5.25	8.75	1.92
AFt-7	72.71	15.64	7.11	4.54	10.22	2.19

Table 3. Results of Deconvolution of C 1s for Aramid Fibers before and after Processing (AF0 and AFt have been Reprinted from Refs 26,27., Pages No Copyright (2024) with Permission from Elsevier)

	relative area of different chemical bonds (%)		
sample	C−C and C═C	O═C−N−H (C═O, C−N)	−COO−
AF0	88.15	11.85	0
AFt	77.14	21.66	1.20
AFt-3	78.93	19.24	1.83
AFt-5	80.23	17.36	2.41
AFt-7	79.53	18.54	1.93

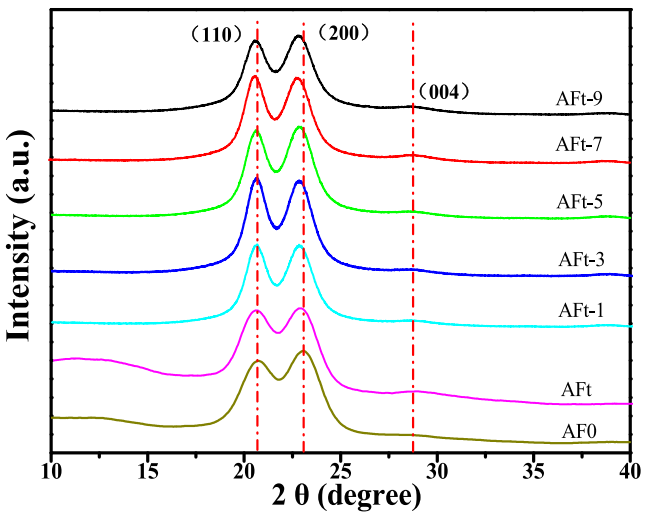

Figure 6. XRD pattern of AFs grafted with different glycidyl POSS contents (AF0 and AFt have been reprinted from refs 26,27., Pages No Copyright (2024) with permission from Elsevier).

normalization method. Table 4 shows the crystallization angles corresponding to each characteristic diffraction peak of AFs. The 2θ values corresponding to (110) and (200) planes slightly shift to a lower angle (Table 4), indicating an increase in the interplanar spacing of the modified specimen and a decrease in the stacked density of microcrystals.[2,24,32] After grafting with a 5% glycidyl POSS solution, the crystallinity of fibers was 83.71%, a 9.91% increase compared to that of AF0.

3.4. TG and DTG Analysis. Figure 7 shows the evolution of weight loss of AFs treated with different glycidyl POSS contents. The final mass residual rate was obtained from Figure 7a. The thermal property of AFt decreased with a final mass residual rate of 58%, possibly because of the oxidation of the benzene ring in the surface molecular chain.[24] Based on the final mass residual rate, the mass of glycidyl POSS grafted on the surface of AFt-1, AFt-3, AFt-5, AFt-7, and AFt-9 was determined to be 1.1, 2.8, 5.4, 8.6, and 9.8%, respectively (Figure 5a). In contrast, the thermal degradation curves of modified fibers reveal two weight losses (Figure 7b). The weight loss from 375 to 520 °C corresponded to the grafted glycidyl POSS on the fiber surface. The modified fibers underwent prominent weight loss from 520 °C because of the decomposition of the macromolecular chains.

As shown in Figure 7b, the maximum decomposition temperature of AF0 is 582.3 °C, whereas that of AFt is 568.2 °C, implying that the oxidation of molecular chains on the fiber surface during thermal oxidation reduced the thermal property of the modified fibers. However, when AFt-1, AFt-3, AFt-5, and AFt-7 were treated with varying glycidyl POSS dosages of 1−9% (Figure 5b), the maximum decomposition temperatures decreased to 570.2, 568.1, 566.4, 561.8, and 555.3 °C, respectively, indicating a reduction in the thermal property due to the graft reaction of glycidyl POSS.

3.5. Morphology Analysis. The surface morphologies of the samples were observed by AFM and scanning electron microscopy (SEM). As can be seen in Figure 8, the untreated fiber (AF0) displayed a smooth surface. Nevertheless, after modification with 3% glycidyl POSS (AFt-3), obvious attachments appeared on the fiber surface. With the modification of 5% glycidyl POSS (AFt-5), the residue on the fiber surface was obvious, and the surface roughness was greatly improved. A large amount of glycidyl POSS was coated on the fiber surface after being soaked in 7 and 9% glycidyl POSS solutions, and then a dense grafted layer was formed. However, the number of active points on the surface of oxidized aramid fiber was limited,[2,33] self-assembly and the grafting reaction occurred simultaneously when 7 and 9%

Table 4. Crystallization Data of Modified AFs (AF0 and AFt have been Reprinted from Refs 26,27., Pages No Copyright (2024) with Permission from Elsevier)[a]

	2θ (deg)		d (Å)		fwhm (deg)			
samples	(110)	(200)	(110)	(200)	(110)	(200)	X_s (nm)	X_c (%)
AF0	20.74	23.05	4.2787	3.8544	1.629	1.699	5.1	76.16
AFt	20.61	22.73	4.3061	3.9601	1.506	1.680	5.4	80.12
AFt-1	20.87	22.74	4.2642	3.8159	1.409	1.562	5.4	81.83
AFt-3	20.88	22.78	4.2571	3.8005	1.415	1.530	5.7	82.79
AFt-5	20.92	22.77	4.2531	3.8001	1.434	1.457	5.9	83.71
AFt-7	20.88	22.78	4.2561	3.7601	1.425	1.629	5.4	83.98
AFt-9	20.94	22.77	4.2709	3.8507	1.504	1.624	5.5	83.97

[a] X_c—crystallinity; d (Å)—interplanar crystal spacing; X_s—average crystallite size; fwhm—peak width at half height.

https://doi.org/10.1021/acsomega.4c00260
ACS Omega 2024, 9, 24489−24499

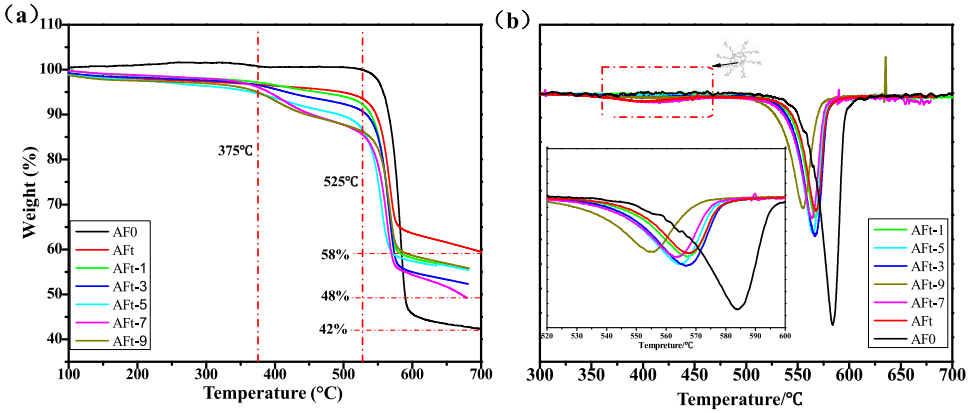

Figure 7. (a) TG and (b) DTG of AFs modified with different glycidyl POSS contents.

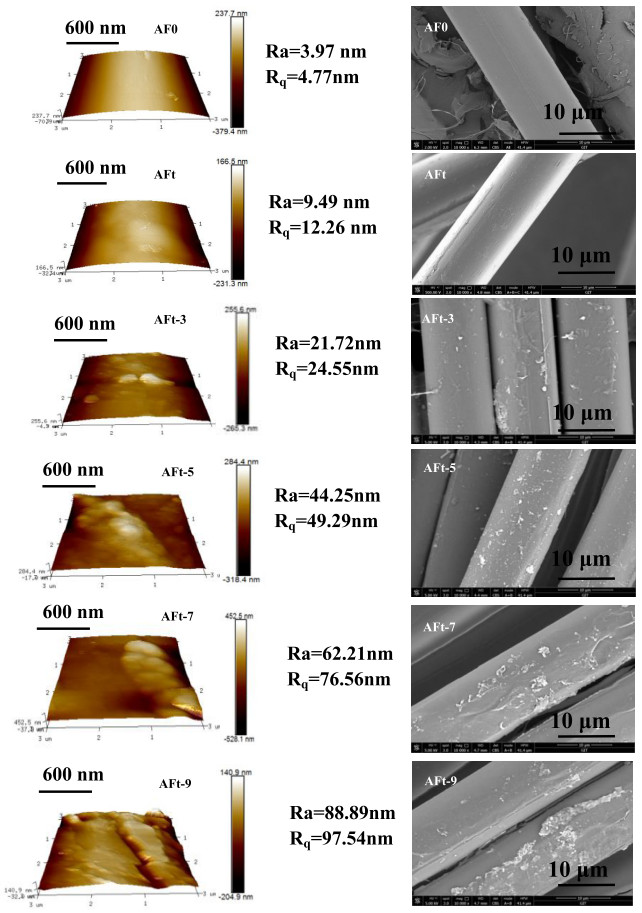

Figure 8. AFM and SEM of modified AFs (AF0 and AFt have been reprinted from refs 26,27., Pages No Copyright (2024) with permission from Elsevier).

glycidyl POSS were introduced, the grafted layer of AFt-5 was more uniform than those of AFt-7 and AFt-9.

3.6. Graft Coating Layer Characterization. The cross sections of single untreated and modified fibers in the matrix of epoxy resin were observed by TEM in order to confirm the thickness of the grafted interface layer. As shown in Figure 9, the surroundings of AF0 were clean and smooth, and the thickness of the grafted interface layer was about 10 nm (Figure 9(a1),(a2)). The oxidation treatment process (AFt) improved the interfacial adhesion with epoxy resin, and the interfacial layer thickness increased.[24] Due to the grafting reaction of glycidyl POSS, the changes in surface morphology and polarity were beneficial to improving their interface adhesion to epoxy resin. There was a dense modified layer around the modified fibers. The thicknesses of the grafted layer on the fiber surfaces of AFt-5 and AFt-7 were about 40 and 80 nm, respectively.

3.7. Mechanical Properties. Fiber tensile tests were performed on single fiber filaments of these five samples to determine the impact of surface modification on their tensile properties. Tensile test results are shown in Figure 10. During thermal oxidation, the aggregate structure on the fiber surface rearranged, and the grain size became larger, which impacted the mechanical properties of AFs.[2,24] Results showed that the mean tensile strength decreased from 23.8 to 22.7 MPa (by 4.6%) after surface modification. The monofilament tensile strength of modified fibers increased with increasing glycidyl POSS dosages. Compared with AF0, the tensile strength of AFt-5 increased by 8.4%. However, a large number of attachments on the surface easily form stress concentration, and the tensile strengths of monofilaments increased by ∼9.6% and 5.8% for AFt-7 and AFt-9, respectively.

3.8. Interfacial Adhesion. Figure 11 intuitively illustrates the SEM photos of modified AF/epoxy resin droplets, and the IFSS values between the modified AFs and epoxy resin droplets are shown in Figure 12. N atoms in the imidazole ring, which acts as a reaction accelerator of 2-ethyl-4-methylimidazole in this paper, open the epoxide group of glycidyl POSS to form a 1:2 addition product. Then, the oxygen anion produced by the epoxy ring opening of glycidyl POSS continues to catalyze the ring opening of the epoxide group and promote the grafting reaction. When the dosage of glycidyl POSS is small, the aramid fiber can be uniformly coated and grafted, while when the dosage of glycidyl POSS is greater than 5%, the coating and self-polymerization are mainly performed. Coating and grafting can improve the surface polarity and roughness of the modified fibers more effectively with the act of 5 wt % glycidyl POSS. Although the monofilament tensile strength of the fibers decreased in Figure 10 for AFt, the increased surface roughness and surface polarity supplied a larger contact area (Figure 11(b)), the increase of the interfacial bonding between aramid fibers and epoxy resin can effectively enhance the mechanical capacity,[24,29,30] and the mean IFSS values of AFt increased to 18.05 MPa.

For composites, the increase in mechanical properties and interfacial adhesion is due to the joint contribution of the

https://doi.org/10.1021/acsomega.4c00260
ACS Omega 2024, 9, 24489−24499

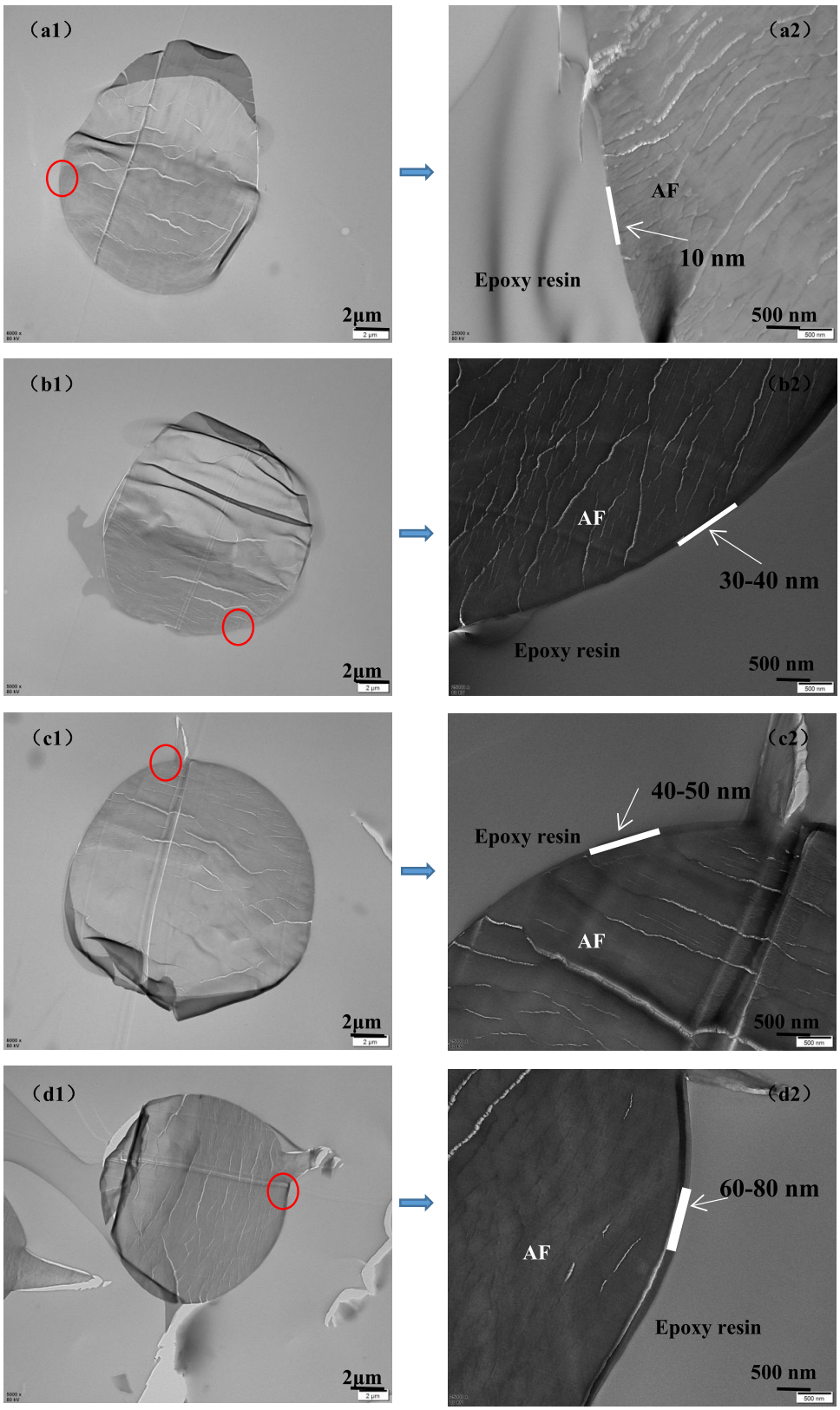

Figure 9. TEM photos of aramid fiber/epoxy composites before and after modification (a1, a2—AF0; b1, b2—AFt; c1, c2—AFt-5; d1, d2—AFt-7).

surface polarity and surface roughness. Li et al.[12] developed a new method to coat polyamide acid (PAA) onto the surface of AF to reinforce the interfacial properties with epoxy resin. The IFSS increased by 40.7% after the treatment with 5 wt % PAA while maintaining the tensile properties of AF. The interfacial adhesion of epoxy and PDA-functionalized AF is improved by 62.5%, as reported by Sa et al.[34] With the increase of tensile strength, surface polarity, and roughness of fiber monofila-

https://doi.org/10.1021/acsomega.4c00260
ACS Omega 2024, 9, 24489−24499

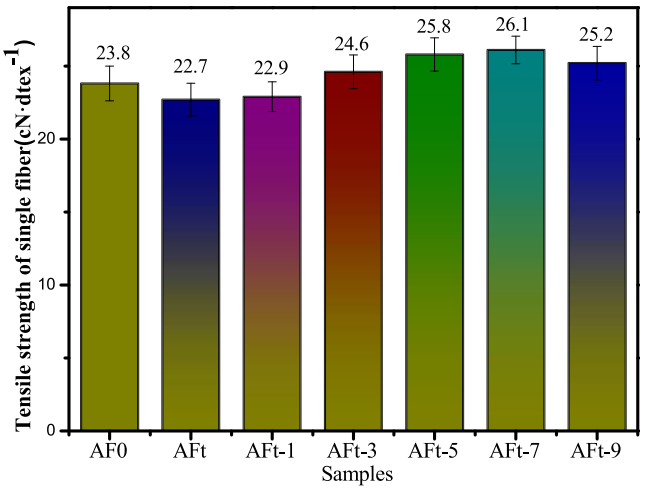

Figure 10. Tensile strength of modified AFs (AF0 and AFt have been reprinted from refs 26,27., Pages No Copyright (2024) with permission from Elsevier.).

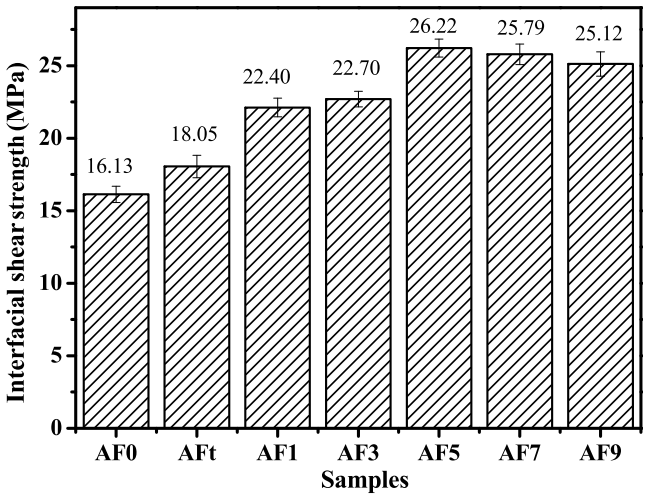

Figure 12. Interface adhesion between the modified AFs and epoxy resin droplets (AF0 and AFt have been reprinted from refs 26,27., Pages No Copyright (2024) with permission from Elsevier).

ments, the interface adhesion between aramid fibers and epoxy resin can be effectively enhanced after glycide POSS grafting, and AFt-5 and AFt-7 show the best performance. The average IFSS values of AFt-5 and AFt-7 were 26.22 and 25.79 MPa, with increases of 62.55 and 59.88%, respectively. However, the surface attachment size of AFt-9 is large, even reaching the micrometer level, which is not conducive to improving the interface bond strength. The mean IFSS value of AFt-9 is 25.12 MPa.

4. CONCLUSIONS

In summary, we have developed a grafted structure on an aramid fiber by combining air oxidation pretreatment and glycidyl POSS impregnation grafting. The polar group produced by oxidation of the benzene ring of aramid fibers during the preoxidation process laid a foundation for the grafting reaction of glycidyl POSS. Glycidyl POSS can undergo an interfacial grafting reaction with aramid fibers, thus improving the surface polarity of the modified AFs further. After grafting with a 5% glycidyl POSS solution, the crystallinity of the fibers was 83.71%, and the tensile strength of the monofilament increased to 25.8 MPa, corresponding to an increase of 8.4%. Due to the production of grafting, the thermal stability of the fiber decreased. In addition to the satisfactory tensile strength of the monofilament, the thickness of the grafted layer was about 30−40 nm in the process of grafting modification with 5% glycidyl POSS. Meanwhile, the IFSS between the fibers modified by 5% glycidyl POSS and epoxy resin increased by 62.55%. Therefore, This study provides a feasible method for interfacial modification of aramid fiber-reinforced epoxy resin composites and further widens the preoxidation treatment as an auxiliary process in the surface modification of AFs.

AUTHOR INFORMATION

Corresponding Author

Le Yang − *School of Materials and Energy Engineering, Guizhou Institute of Technology, Guiyang 550003, China; Guizhou Colleges and Universities Process Industry New Process Engineering Research Center, Guiyang 550003, China;* orcid.org/0000-0002-7613-211X; Email: yangle1990@git.edu.cn

Authors

Yang Li − *School of Materials and Energy Engineering, Guizhou Institute of Technology, Guiyang 550003, China; Guizhou Colleges and Universities Process Industry New Process Engineering Research Center, Guiyang 550003, China*

Caiwen Shi − *School of Materials and Energy Engineering, Guizhou Institute of Technology, Guiyang 550003, China*

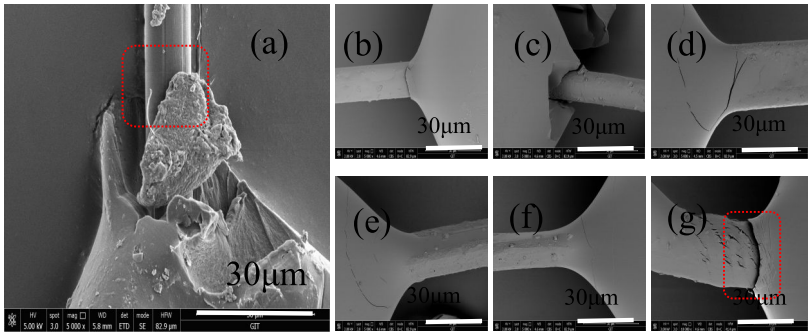

Figure 11. SEM photos of modified AF/epoxy resin droplets (AF0 and AFt have been reprinted from refs 26,27., Pages No Copyright (2024) with permission from Elsevier). a—AF0; b—AFt; c—AFt-1; d—AFt-3; e—AFt-5; f—AFt-7; and g—AFt-9.

https://doi.org/10.1021/acsomega.4c00260
ACS Omega 2024, 9, 24489−24499

Xiaoli Pan − *School of Materials and Energy Engineering, Guizhou Institute of Technology, Guiyang 550003, China*
Ziyi Wang − *School of Materials and Energy Engineering, Guizhou Institute of Technology, Guiyang 550003, China*

Complete contact information is available at: https://pubs.acs.org/10.1021/acsomega.4c00260

Author Contributions

Y.L.: conceptualization, methodology, and writing—original draft. C.S.: resources and methodology. X.P.: conceptualization. L.Y.: writing—review. Z.W.: editing, validation, and resources.

Notes

The authors declare no competing financial interest.

■ ACKNOWLEDGMENTS

The authors gratefully acknowledge the National Natural Science Foundation of China (Grant No. 52363009) and PhD start-up fund of Guizhou Institute of Technology and Guizhou Colleges and Universities Process Industry New Process Engineering Research Center (Qian Jiao Ji [2022] 034).

■ REFERENCES

(1) Wagih, A.; Sebaey, T. A.; Yudhanto, A.; Lubineau, G. Post-impact flexural behavior of carbon-aramid/epoxy hybrid composites. *Compos. Struct.* **2020**, *239*, No. 112022.
(2) Zhang, B.; Jia, L. H.; Tian, M.; Ning, N. Y.; Zhang, L. Q.; Wang, W. C. Surface and interface modification of aramid fiber and its reinforcement for polymer composites: a review. *Eur. Polym. J.* **2021**, *147*, No. 110352.
(3) Enew, A. M.; Elfattah, M. A.; Fouda, S. R.; Hawash, S. A. Effect of aramid and carbon fibers with nano carbon particles on the mechanical properties of EPDM rubber thermal insulators for solid rocket motors application. *Polym. Test.* **2021**, *103*, No. 107341.
(4) Zhong, J. C.; Luo, Z.; Hao, Z.; Guo, Y. L.; Zhou, Z. T.; Li, P.; Xue, B. Enhancing fatigue properties of styrene butadiene rubber composites by improving interface adhesion between coated aramid fibers and matrix. *Composites, Part B* **2019**, *172*, 485−495.
(5) Zhang, B.; Wang, W.; Tian, M.; Ning, N.; Zhang, L. Preparation of aramid nanofiber and its application in polymer reinforcement: a review. *Eur. Polym. J.* **2020**, *139*, No. 109996.
(6) Zuo, L. S.; Li, K.; Ren, D. G.; Xu, M. Z.; Tong, L. F.; Liu, X. B. Surface modification of aramid fiber by crystalline polyarylene ether nitrile sizing for improving interfacial adhesion with polyarylene ether nitrile. *Composites, Part B* **2021**, *217*, No. 108917.
(7) Randall, J. D.; Eyckens, D. J.; Servinis, L.; Stojcevski, F.; O'Dell, L. A.; Gengenbach, T. R.; Demir, B.; Walsh, T. R.; Henderson, L. C. Designing carbon fiber composite interfaces using a 'graft-to' approach: surface grafting density versus interphase penetration. *Carbon* **2019**, *146*, 88−96.
(8) Zhang, B.; Lian, T.; Shao, X.; Tian, M.; Ning, N.; Zhang, L.; Wang, W. Surface coating of aramid fiber by a graphene/aramid nanofiber hybrid material to enhance interfacial adhesion with rubber matrix. *Ind. Eng. Chem. Res.* **2021**, *60*, 2472−2480.
(9) Zhang, S. H.; Li, M. Z.; Cheng, K.; Lu, S. J. A facile method to prepare peg coatings on the fiber surface by the reconstruction of hydrogen bonds for enhancing the interfacial strength of fibers and resins. *Colloids Surf., A* **2020**, *589*, No. 124426.
(10) Sun, Z.; Zhou, Y.; Li, W.; Chen, S.; You, S.; Ma, J. Preparation of silver-plated para-aramid fiber by employing low-temperature oxygen plasma treatment and dopamine functionalization. *Coatings* **2019**, *9*, No. 599.
(11) Fan, W.; Tian, H.; Wang, H.; Zhang, T.; Yang, X.; Yu, Y.; Meng, X.; Yu, X.; Yuan, L.; Xu, B.; Wang, S. Enhanced interfacial adhesion of aramid fiber iii reinforced epoxy composites via low temperature plasma treatment. *Polym. Test.* **2018**, *72*, 147−156.
(12) Li, Y.; Luo, Z.; Yang, L.; Luo, Y. M.; Li, Q.; Zhang, L. Y.; Xiang, K. Influence of polyamide acid coating reaction on the properties of aramid fibre. *Polymer* **2019**, *178*, No. 121550.
(13) Chen, J. R.; Zhu, Y. F.; Ni, Q. Q.; Fu, Y.; Fu, X. Surface modification and characterization of aramid fibers with hybrid coating. *Appl. Surf. Sci.* **2014**, *321*, 103−108.
(14) Yuan, H.; Wang, W. C.; Yang, D. Z.; Zhou, X.; Zhao, Z. Z.; Zhang, L.; Wang, S.; Feng, J. Hydrophilicity modification of aramid fiber using a linear shape plasma excited by nanosecond pulse. *Surf. Coat. Technol.* **2018**, *344*, 614−620.
(15) Wang, F.; Wu, Y. D.; Huang, Y. D. High strength, thermostable and fast-drying hybrid transparent membranes with POSS nanoparticles aligned on aramid nanofibers. *Composites, Part A* **2018**, *110*, 154−161.
(16) Lv, J. W.; Liu, Y. H.; Qin, Y. T.; Yin, Q.; Chen S, Y.; Cheng, Z.; Yin, J. Y.; Yu Dai, Y.; Liu, W.; Liu, X. H. Constructing "Rigid-and-Soft" interlocking stereoscopic interphase structure of aramid fiber composites with high interfacial shear strength and toughness. *Composites, Part A* **2021**, *145*, No. 106386.
(17) Yazıcı, N.; Dursun, S.; Yarıcı, T.; Kılıç, B.; Arıcan, M. O.; Mert, O.; Karaağaç, B.; Özkoç, G.; Kodal, M. The outstanding interfacial adhesion between acrylo-poss/natural rubber composites and polyamide-based cords: 'an environmentally friendly alternative to resorcinol-formaldehyde latex coating. *Polymer* **2021**, *228*, No. 123880.
(18) Zhou, L.; Yuan, L.; Guan, Q.; Gu, A.; Liang, G. Building unique surface structure on aramid fibers through a green layer-by-layer self-assembly technique to develop new high performance fibers with greatly improved surface activity, thermal resistance, mechanical properties and UV resistance. *Appl. Surf. Sci.* **2017**, *411*, 34−45.
(19) Cao, C.; Peng, J. S.; Liang, X. M.; Saiz, E.; Wolf, S. E.; Wagner, H. D.; Jiang, L.; Cheng, Q. F. Strong, conductive aramid fiber functionalized by graphene. *Composites, Part A* **2021**, *140*, No. 106161.
(20) Zeng, S. L.; Zhang, T. R.; Nie, M.; Fei, G. X.; Wang, Q. Effect of root-like mechanical-interlocking interface in polypropylene/aramid fiber composites from experimental to numerical study. *Composites, Part B* **2021**, *216*, No. 108868.
(21) Chen, J. Y.; Zhao, L. H.; Zhou, K. Improvement in the mechanical performance of multi jet fusion-printed aramid fiber/polyamide 12 composites by fiber surface modification. *Addit. Manuf.* **2022**, *51*, No. 102576.
(22) Eyckens, D. J.; Jarvis, K.; Barlow, A. J.; Yin, Y.; Soulsby, L. C.; Athulya Wickramasingha, Y.; Stojcevski, F.; Andersson, G.; Francis, P. S.; Henderson, L. C. Improving the effects of plasma polymerization on carbon fiber using a surface modification pretreatment. *Composites, Part A* **2021**, *143*, No. 106319.
(23) Mengjin, W.; Lixia, J.; Suling, L.; Zhigang, Q.; Sainan, W.; Ruosi, Y. Interfacial performance of high-performance fiber-reinforced composites improved by cold plasma treatment: a review. *Surf. Interfaces* **2021**, *24*, No. 101077.
(24) Li, Y.; Luo, Z.; Yang, L.; Li, X. L.; Xiang, K. Study on surface properties of aramid fiber modified in supercritical carbon dioxide by glycidyl-POSS. *Polymers* **2019**, *11*, No. 700.
(25) Zuo, L. S.; Li, K.; Ren, D. X.; Xu, M. Z.; Tong, L. F.; Liu, X. B. Surface modification of aramid fiber by crystalline polyarylene ether nitrile sizing for improving interfacial adhesion with polyarylene ether nitrile. *Composites, Part B* **2021**, *217*, No. 108917.
(26) Li, Y.; Xie, G. Y.; Li, R.; Wu, Y. J.; Chen, C. Q.; Luo, Z. Supercritical carbon dioxide assisted impregnation and graft of polyamide acid into aramid fiber for formation of polar interface. *J. Mater. Res. Technol.* **2022**, *21*, 1−11.
(27) Wu, K.; Wang, X. Y.; Xu, Y. H.; Guo, W. H. Flame retardant efficiency of modified para-aramid fiber synergizing with ammonium polyphosphate on PP/EPDM. *Polym. Degrad. Stab.* **2020**, *172*, No. 109065.
(28) Liu, F. F.; Guo, H. Q.; Zhao, Y.; Qiu, X. Q.; Gao, L. X. Enhanced resistance to the atomic oxygen exposure of POSS/

polyimide composite fibers with surface enrichment through wet spinning. *Eur. Polym. J.* **2018**, *105*, 115−125.
(29) Ma, Y. L.; He, L. POSS-pendanted in epoxy chain inorganic-organic hybrid for highly thermo-mechanical, permeable and hydrothermal-resistant coatings. *Mater. Chem. Phys.* **2017**, *201*, 120−129.
(30) Wu, G. S.; Ma, L.; Wang, Y. W.; Liu, L.; Huang, Y. D. Interfacial properties and impact toughness of methylphenylsilicone resin composites by chemically grafting POSS and tetraethylenepentamine onto carbon fibers. *Composites, Part A* **2016**, *84*, 1−8.
(31) Yin, L. P.; Luo, Z.; Zhong, J. C.; Yan, B.; Ji, Y. C. Behaviour and mechanism of fatigue crack growth in aramid-fibre reinforced styrene-butadiene rubber composites. *Int. J. Fatigue* **2020**, *134*, No. 105502.
(32) Gao, D. G.; Li, X. J.; Cheng, Y. M.; Lyu, B.; Ma, J. Z. The modification of collagen with biosustainable POSS graft oxidized sodium alginate composite. *Int. J. Biol. Macromol.* **2022**, *200*, 557−565.
(33) Xue, C. H.; Fan, Q. Q.; Guo, X. J.; An, Q. F.; Jia, S. T. Fabrication of superhydrophobic cotton fabrics by grafting of POSS-based polymers on fibers. *Appl. Surf. Sci.* **2019**, *465*, 241−248.
(34) Sa, R.; Yan, Y.; Wei, Z. H.; Zhang, L. Q.; Wang, W. C.; Tian, M. Surface modification of aramid fibers by bio-inspired poly(dopamine) and epoxy functionalized silane grafting. *ACS Appl. Mater. Interfaces* **2014**, *6* (23), 21730−21738.

https://doi.org/10.1021/acsomega.4c00260
ACS Omega 2024, 9, 24489−24499